

Few-layer black phosphorus based saturable absorber mirror for pulsed solid-state lasers

Jie Ma,¹ Shunbin Lu,² Zhinan Guo,² Xiaodong Xu,³ Han Zhang,^{2,4} Dingyuan Tang,^{1,5}
and Dianyuan Fan²

¹*School of Electrical and Electronic Engineering, Nanyang Technological University, Singapore 639798, Singapore*

²*SZU-NUS Collaborative Innovation Centre for Optoelectronic Science & Technology, and Key Laboratory of Optoelectronic Devices and Systems of Ministry of Education and Guangdong Province, Shenzhen University, Shenzhen, China*

³*School of Physics and Electronic Engineering, Jiangsu Normal University, Xuzhou 221116, China*

⁴*hzhang@szu.edu.cn*

⁵*EDYTang@ntu.edu.sg*

Abstract: We experimentally demonstrated that few-layer black phosphorus (BP) could be used as an optical modulator for solid-state lasers to generate short laser pulses. The BP flakes were fabricated by the liquid phase exfoliation method and drop-casted on a high-reflection mirror to form a BP-based saturable absorber mirror (BP-SAM). Stable Q-switched pulses with a pulse width of 620 ns at the wavelength of 1046 nm were obtained in a Yb:CaYAlO₄ (Yb:CYA) laser with the BP-SAM. The generated pulse train has a repetition rate of 113.6 kHz and an average output power of 37 mW. Our results show that the BP-SAMs could have excellent prospective for ultrafast photonics applications.

©2015 Optical Society of America

OCIS codes: (160.4330) Nonlinear optical materials; (160.4236) Nanomaterials; (140.3580) Lasers, solid-state; (140.3540) Lasers, Q-switched.

References and links

1. K. S. Novoselov, A. K. Geim, S. V. Morozov, D. Jiang, Y. Zhang, S. V. Dubonos, I. V. Grigorieva, and A. A. Firsov, "Electric Field Effect in Atomically Thin Carbon Films," *Science* **306**(5696), 666–669 (2004).
2. K. K. Kim, A. Hsu, X. Jia, S. M. Kim, Y. Shi, M. Hofmann, D. Nezich, J. F. Rodriguez-Nieva, M. Dresselhaus, T. Palacios, and J. Kong, "Synthesis of monolayer hexagonal boron nitride on cu foil using chemical vapor deposition," *Nano Lett.* **12**(1), 161–166 (2012).
3. M. Chhowalla, H. S. Shin, G. Eda, L.-J. Li, K. P. Loh, and H. Zhang, "The chemistry of two-dimensional layered transition metal dichalcogenide nanosheets," *Nat. Chem.* **5**(4), 263–275 (2013).
4. L. Li, Y. Yu, G. J. Ye, Q. Ge, X. Ou, H. Wu, D. Feng, X. H. Chen, and Y. Zhang, "Black phosphorus field-effect transistors," *Nat. Nanotechnol.* **9**(5), 372–377 (2014).
5. H. Liu, A. T. Neal, Z. Zhu, Z. Luo, X. Xu, D. Tománek, and P. D. Ye, "Phosphorene: An unexplored 2D semiconductor with a high hole mobility," *ACS Nano* **8**(4), 4033–4041 (2014).
6. J. R. Brent, N. Savjani, E. A. Lewis, S. J. Haigh, D. J. Lewis, and P. O'Brien, "Production of few-layer phosphorene by liquid exfoliation of black phosphorus," *Chem. Commun. (Camb.)* **50**(87), 13338–13341 (2014).
7. P. Yasaei, B. Kumar, T. Foroozan, C. Wang, M. Asadi, D. Tuschel, J. E. Indacochea, R. F. Klie, and A. Salehi-Khojin, "High-quality black phosphorus atomic layers by liquid-phase exfoliation," *Adv. Mater.* **27**(11), 1887–1892 (2015).
8. J. Qiao, X. Kong, Z.-X. Hu, F. Yang, and W. Ji, "High-mobility transport anisotropy and linear dichroism in few-layer black phosphorus," *Nat. Commun.* **5**, 4475 (2014).
9. V. Tran, R. Soklaski, Y. Liang, and L. Yang, "Layer-controlled band gap and anisotropic excitons in few-layer black phosphorus," *Phys. Rev. B* **89**(23), 235319 (2014).
10. T. Low, R. Roldán, H. Wang, F. Xia, P. Avouris, L. M. Moreno, and F. Guinea, "Plasmons and screening in monolayer and multilayer black phosphorus," *Phys. Rev. Lett.* **113**(10), 106802 (2014).
11. S. P. Koenig, R. A. Doganov, H. Schmidt, A. H. Castro Neto, and B. Özyilmaz, "Electric field effect in ultrathin black phosphorus," *Appl. Phys. Lett.* **104**(10), 103106 (2014).
12. F. Xia, H. Wang, and Y. Jia, "Rediscovering black phosphorus as an anisotropic layered material for optoelectronics and electronics," *Nat. Commun.* **5**, 4458 (2014).
13. S. B. Lu, L. L. Miao, Z. N. Guo, X. Qi, C. J. Zhao, H. Zhang, S. C. Wen, D. Y. Tang, and D. Y. Fan, "Broadband nonlinear optical response in multi-layer black phosphorus: an emerging infrared and mid-infrared optical material," *Opt. Express* **23**(9), 11183–11194 (2015).
14. H. Wang, X. Wang, F. Xia, L. Wang, H. Jiang, Q. Xia, M. L. Chin, M. Dubey, and S. J. Han, "Black Phosphorus Radio-Frequency Transistors," *Nano Lett.* **14**(11), 6424–6429 (2014).

15. M. Buscema, D. J. Groenendijk, S. I. Blanter, G. A. Steele, H. S. J. van der Zant, and A. Castellanos-Gomez, "Fast and broadband photoresponse of few-layer black phosphorus field-effect transistors," *Nano Lett.* **14**(6), 3347–3352 (2014).
16. Y. Chen, G. Jiang, S. Chen, Z. Guo, X. Yu, C. Zhao, H. Zhang, Q. Bao, S. Wen, D. Tang, and D. Fan, "Mechanically exfoliated black phosphorus as a new saturable absorber for both Q-switching and Mode-locking laser operation," *Opt. Express* **23**(10), 12823–12833 (2015).
17. J. Sotor, G. Sobon, W. Macherzynski, P. Paletko, and K. M. Abramski, "Black phosphorus-a new saturable absorber material for ultrashort pulse generation," arXiv: 1504.04731 (2015).
18. T. Jiang, K. Yin, X. Zheng, H. Yu, and X. A. Cheng, "Black phosphorus as a new broadband saturable absorber for infrared passively Q-switched fiber lasers," arXiv:1504.07341 (2015).
19. D. Li, H. Jussila, L. Karvonen, G. J. Ye, H. Lipsanen, X. H. Chen, and Z. P. Sun, "Ultrafast pulse generation with black phosphorus," arXiv: 1505.00480 (2015).
20. Z. C. Luo, M. Liu, Z. N. Guo, X. F. Jiang, A. P. Luo, C. J. Zhao, X. F. Yu, W. C. Xu, and H. Zhang, "Micofiber-based few-layer black phosphorus saturable absorber for ultra-fast fiber laser," arXiv: 1505.03035 (2015).
21. J. M. Dawlaty, S. Shivaraman, J. Strait, P. George, M. Chandrashekhara, F. Rana, M. G. Spencer, D. Veksler, and Y. Chen, "Measurement of the optical absorption spectra of epitaxial graphene from terahertz to visible," *Appl. Phys. Lett.* **93**(13), 131905 (2008).
22. R. R. Nair, P. Blake, A. N. Grigorenko, K. S. Novoselov, T. J. Booth, T. Stauber, N. M. R. Peres, and A. K. Geim, "Fine structure constant defines visual transparency of graphene," *Science* **320**(5881), 1308 (2008).
23. H. Yu, X. Chen, H. Zhang, X. Xu, X. Hu, Z. Wang, J. Wang, S. Zhuang, and M. Jiang, "Large energy pulse generation modulated by graphene epitaxially grown on silicon carbide," *ACS Nano* **4**(12), 7582–7586 (2010).
24. C. Gao, R. Wang, L. Zhu, M. Gao, Q. Wang, Z. Zhang, Z. Wei, J. Lin, and L. Guo, "Resonantly pumped 1.645 μm high repetition rate Er:YAG laser Q-switched by a graphene as a saturable absorber," *Opt. Lett.* **37**(4), 632–634 (2012).
25. G. Q. Xie, J. Ma, P. Lv, W. L. Gao, P. Yuan, L. J. Qian, H. H. Yu, H. J. Zhang, J. Y. Wang, and D. Y. Tang, "Graphene saturable absorber for Q-switching and mode locking at 2 μm wavelength [Invited]," *Opt. Mater. Express* **2**(6), 878–883 (2012).
26. Y. Tan, C. Cheng, S. Akhmedaliev, S. Zhou, and F. Chen, "Nd:YAG waveguide laser Q-switched by evanescent-field interaction with graphene," *Opt. Express* **22**(8), 9101–9106 (2014).
27. A. Butler, D. Spence, and D. Coutts, "Scaling Q-switched microchip lasers for shortest pulses," *Appl. Phys. B* **109**(1), 81–88 (2012).
28. D. Sebbag, A. Korenfeld, U. Ben-Ami, D. Elooz, E. Shalom, and S. Noach, "Diode end-pumped passively Q-switched Tm:YAP laser with 1.85-mJ pulse energy," *Opt. Lett.* **40**(7), 1250–1253 (2015).

1. Introduction

Two-dimensional nano-materials, such as graphene [1], hexagonal boron nitride (hBN) [2], and transition metal dichalcogenides (TMDs) [3], have attracted significant attention in recent years due to their outstanding physical and chemical properties, as well as exciting applications in various fields. Very recently, phosphorene, another attractive two-dimensional semiconductor nanomaterial, which was a single layer of black phosphorus (BP) arranged in a puckered honeycomb structure with out of plane ridges, was successfully fabricated [4–7]. It has been demonstrated that monolayer phosphorene has direct bandgap [4], high in-plane anisotropy [5,8,9], high carrier mobility (up to $\sim 1,000 \text{ cm}^2\text{V}^{-1}\text{s}^{-1}$) [4,10,11], and large on/off ratios ($>10^5$) at the room temperature [4,12], making it a suitable alternative two-dimensional semiconductor material for electronics and optoelectronics applications. Moreover, previous theoretical and experimental studies have shown that the bandgap of BP strongly depends on the layer number, ranging from $\sim 2.0 \text{ eV}$ for monolayer to $\sim 0.3 \text{ eV}$ for bulk due to the layer–layer coupling [8,13]. Such a thickness-dependent direct bandgap feature may lead to wide range potential photonics applications in the wavelength range from $\sim 600 \text{ nm}$ to $\sim 4 \mu\text{m}$. In addition, broadband nonlinear optical response from 400 nm to 1930 nm of multilayer BP was successfully demonstrated recently by Lu et. al [13]. These results indicate that BP films could be exploited as ultra-fast nonlinear photonics devices, such as the Q-switcher and mode-locker for pulse lasers over an ultrawide spectral range from visible to infrared. However, so far most of the studies on BP atomic layers were focused on the field-effect transistors [4,14,15]. There are only a few reports about the BP saturable absorbers, but mainly for the pulsed fiber lasers at around $1.5 \mu\text{m}$ and $2 \mu\text{m}$ [16–20].

Up to now, the Q-switching and mode-locking are two mainstream laser techniques for generating short laser pulses. Compared to mode-locking, Q-switching technique can generate pulses with much larger pulse energy, lower pulse repetition rate, and longer pulse duration. It has been widely used in the fields of medical treatment, material processing, range finding,

environmental sensing, and non-linear frequency conversion where reliable and cost-effective nanosecond laser pulses are required. Generally, passive Q-switching operation of lasers is mainly achieved with the conventional saturable absorbers, such as GaAs, Cr:YAG, SESAM, Cr:ZnS, which are sensitive to the laser operation wavelength. Due to its wavelength-independent property [21,22], graphene was ever considered as a very promising broadband saturable absorber for Q-switching lasers and has been intensively investigated in recent years [23–26]. However, monolayer graphene has very low optical modulation depth due to its weak absorption on the incident light. Till now most of the Q-switched pulses generated with the graphene Q-switcher cannot compete with those generated with the conventional saturable absorbers in terms of the pulse duration and energy [27,28].

In this letter, we demonstrate that few-layer BP fabricated by the liquid phase exfoliation method can be used as a saturable absorber to generate short pulses in solid-state lasers. The BP flakes were drop-casted on a high-reflection mirror to form a BP-SAM. With the BP-SAM in a diode pumped Yb:CYA laser, stable Q-switched pulses with a pulse width of 620 ns and central wavelength at 1046 nm were successfully obtained. The Q-switched pulse train has an average output power of 39 mW and a repetition rate of 113.6 kHz. The experimental result shows that BP could be an effective saturable absorber for solid-state lasers.

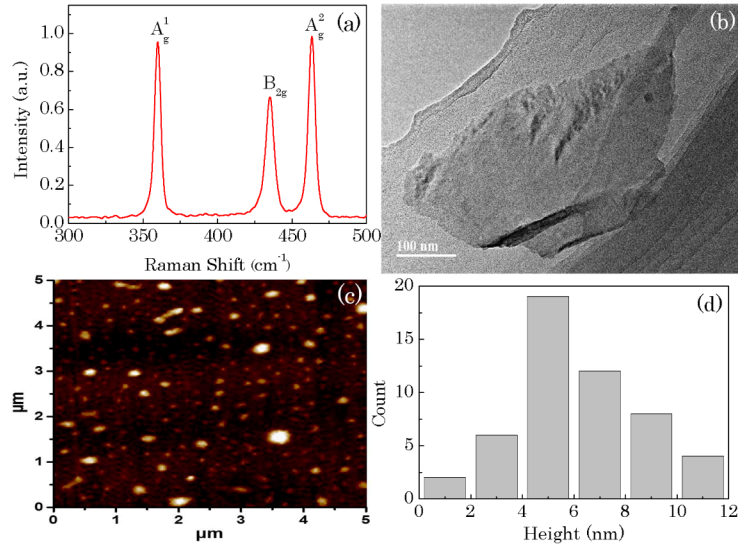


Fig. 1. Characterization of the liquid-phase-exfoliated BP nanoflakes. (a) Raman spectrum of the prepared few-layer BP nanoflakes; (b) TEM image of the as-prepared few-layer BP nanoflakes; (c) 2D topographical AFM image of the as-prepared few-layer BP nanoflakes; (d) Histogram of thickness distribution of the BP nanoflakes.

In the experiment the few-layer BP nanoflakes were fabricated by the liquid-phase exfoliation technique which was widely used for large-scale production of the two-dimensional nano-materials, such as graphene, hBN, and TMDs [6]. The BP bulk crystal (Smart Elements, purity 99.998%) was exfoliated and dispersed into N-methylpyrrolidone (NMP) solvent and ultra-sonicated for 4 hours. Thin BP nanoflakes were formed in the solution due to the breaking down of the inter-layer van der Waals bonding by the ultrasonic energy. The dispersion was centrifuged at a speed of 1500 rpm for 45 minutes to remove the large number of thick flakes. After that, the obtained few-layer BP was transferred into ethanol from the dispersion. Then the BP-SAM was fabricated by drop-casting the collected BP dispersion on a high-reflection plane mirror and dried in a vacuum oven. Figure 1 (a) shows the Raman spectrum of the fabricated BP nanoflakes excited by a 633 nm laser source. Three obvious peaks at $\sim 360.5 \text{ cm}^{-1}$, $\sim 435.1 \text{ cm}^{-1}$, and $\sim 463.5 \text{ cm}^{-1}$, corresponding to the characteristic modes A_g^1 , B_{2g} , and A_g^2 of few-layer BP could be observed. In order to

characterize the as-prepared BP nanoplatelets, the transmission electron microscopy (TEM) and atomic force microscopy (AFM) measurement of the BP nanoplatelets were performed in the experiment. It is to see from the TEM image that the BP nanoplatelets have platelet-like structures with a size not less than several-hundred nanometers, as shown in Fig. 1(b). And the size distribution of the fabricated BP nanoplatelets is mostly in the range from about 180 nm to 600 nm. Figure 1(c) shows the 2D topographical images of the as-prepared BP nanoplatelets located on the silicon substrate. To analyze the thickness of the BP sample, 50 different positions in Fig. 1(c) were chosen for statistics. Figure 1(d) illustrates the statistical histogram on thickness distribution of the BP nanoflakes. It can be seen that most of the nanoplatelets have a thickness between 3 nm to 9 nm. Considering the theoretical thickness value of 0.6 nm for single layer BP [5], the BP nanoplatelets are about 5-15 layers thick in our experiments.

2. Experimental setup and results

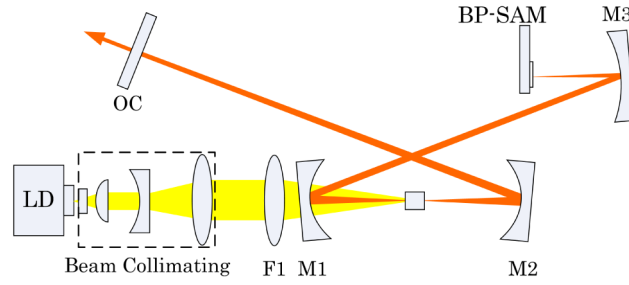


Fig. 2. The schematic of the Q-switched laser setup based on BP-SAM.

The schematic of the passively Q-switched Yb:CYA solid state laser is shown in Fig. 2. An X-folded five-mirror cavity was used in the experiment. The laser gain material was an a-cut Yb:CYA crystal with a Yb^{3+} concentration of 8 at. % in the melt. The crystal was grown by the Czochralski method and cut into dimensions of 3.0 mm in length and $3.0 \times 3.0 \text{ mm}^2$ in cross-section. To minimize the Fresnel reflection losses, the sample was antireflection-coated for both the pump and laser wavelengths. The crystal was wrapped with indium foil and tightly mounted in a water-cooled copper block that is maintained at 20.0°C for effectively removing the heat. A distributed Bragg reflector (DBR) tapered diode laser at 980 nm was used as the pump source. The pump light was first shaped by a home-made laser beam collimating system, and then focused into the crystal via a spherical convex lens (F1) with a focal length of 80 mm. The focused spot size was measured as $\sim 30 \mu\text{m}$ in diameter by a laser beam profiler. The concave mirrors M1 and M2 have the same radius of curvature (ROC) of -50 mm , and M3 has a ROC of -100 mm . They all were high reflection coated at the laser wavelength and anti-reflection coated at the pump wavelength. The laser crystal was placed near the middle of M1 and M2 in the cavity. By ABCD matrix calculation the laser mode diameter was estimated as $\sim 28 \mu\text{m}$ in the Yb:CYA crystal and $\sim 120 \mu\text{m}$ on the BP-SAM. The as-fabricated BP-SAM was also used as the end mirror of the cavity. The plano-plano output coupler has a transmission of 1% from 1000 nm to 1200 nm.

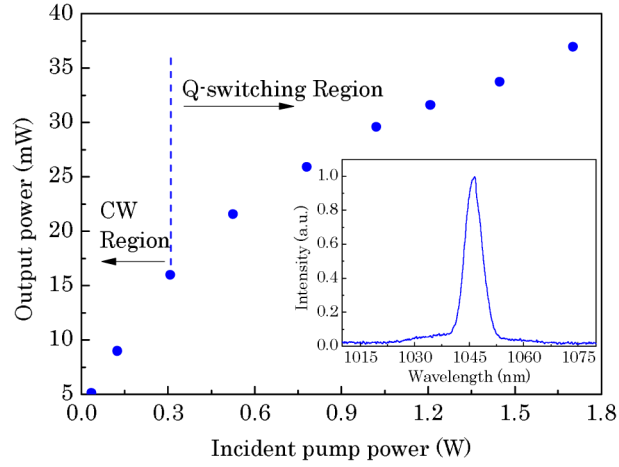


Fig. 3. Output power versus incident pump power of the Q-switched laser.

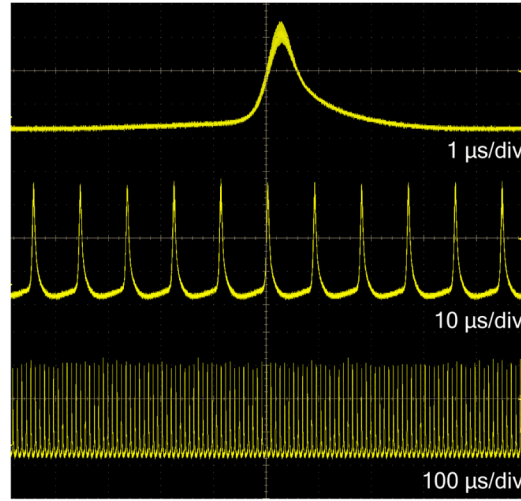


Fig. 4. Typical Q-switched pulses at different time scale under the 1.70 W pump power of the Q-switched laser.

Through carefully aligning the laser cavity and optimizing the laser spot position on the BP-SAM, stable Q-switched operation could be achieved in the laser. Initially, the laser was in the continuous-wave (CW) operation regime. When the pump power was increased to ~ 0.308 W, the laser emission suddenly changed from the CW operation to the Q-switched operation, and the corresponding output power was about 16 mW. Further increasing the incident pump power to ~ 1.70 W, the average output power reached the maximum value of 37 mW. Figure 3 shows the relation of the average output power with the incident pump power. The center wavelength of the Q-switched pulses was at 1046 nm, measured by a USB 4000 spectrometers (Ocean Optics) as shown in the inset of Fig. 3. The Q-switched pulse trains were monitored by a high-speed photo-detector (New Focus, 1611) together with a digital oscilloscope of 1 GHz bandwidth (Tektronix, DPO7104). Figure 4 shows a typical Q-switched pulse train measured with different time scales under 1.70 W pump power. Very stable Q-switched pulses were achieved in the experiment. The Q-switched pulse width and repetition rate varies with the incident pump power, as shown in Fig. 5. When the pump power increased from the Q-switching threshold of 0.308 W to 1.70 W, the pulse width dropped from ~ 1.2 μ s to ~ 620 ns, and the pulse repetition rate changed from ~ 87.7 kHz to

113.6 kHz. Under even higher pumping power the Q-switched pulse train became unstable, where disordered pulses with significant pulse jitter were observed. Based on the obtained average output power and repetition rate, the maximum Q-switched pulse energy was estimated as ~ 325.7 nJ, and maximum peak intensity on the BP-SAM was estimated as 465 kW/cm². No damage was observed on the BP-SAM when the laser was operated under the maximum average output power. During the experiment, we also tried to shift the laser spot out of the drop-casted BP region on the BP-SAM by moving the BP-SAM in the transverse direction, which did not change the cavity configuration. The laser then became CW emission and no Q-switched pulse was obtained, and in the meantime the average output power increased to about 177 mW, demonstrating the existence of non-saturable absorption of the BP-SAM. In addition, we did not observe mode-locking signal in the experiment under the maximum average output power. According to the experimental results and previous works [13, 16], we estimate that the saturation intensity of BP-SAM should be more than 1 MW/cm².

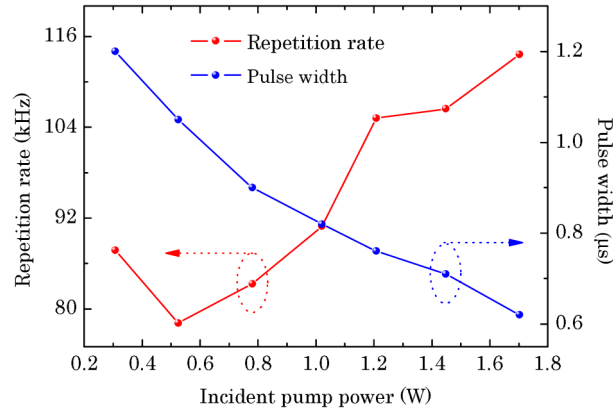


Fig. 5. Pulse width and repetition rate versus the incident pump power.

3. Conclusion

In conclusion, we have experimentally demonstrated that the few-layer BP can be used as a saturable absorber for solid-state lasers to generate short pulses. A fabricated BP-SAM was successfully applied in a diode-pumped Yb:CYA laser to generate 620 ns Q-switched pulses. The Q-switched pulse train has a maximum average power of 37 mW and a repetition rate of 113.6 kHz. To the best of our knowledge, this is the first experimental demonstration of a passively Q-switched solid-state laser with a BP-SAM. Considering that BP has a wide-range thickness-dependent bandgap from ~ 0.3 eV to ~ 2.0 eV, we believe that BP could be a potential broadband saturable absorber for pulse solid state lasers of various wavelengths.

Acknowledgments

The research is partially supported by the funds of Ministry of Education (MOE) Singapore, under Grant No. 35/12, Priority Academic Program Development of Jiangsu Higher Education Institutions (PADP), China, and the National Natural Science Fund of China (Grant No. 61222505, 61435010).